Supplementary Information 2: Model development

S-ketamine model

For the development of *S*-ketamine model, a sequential approach was used in which optimum number of compartments for describing the disposition kinetics of *S*-ketamine were established at first. A three compartmental mammillary model, with one central and two peripheral compartments with separate distributional clearances, was observed to best describe *S*-ketamine concentration time data (ΔOFV = -598), better than a two compartmental model (ΔOFV = -578) or one compartmental model. Three compartmental model also showed an adequate level of precision in the model predicted parameter estimates.

The absorption profile of *S*-ketamine was adequately described by a standard first order absorption process. A transit compartmental model and a single Weibull absorption function were also tested for this purpose, but a linear first order rate constant described the rapid absorption profile of *S*-ketamine with precision and plausible parameter estimates. Use of a single Weibull absorption function resulted in high %RSE levels in the model parameter estimates, especially the shape factor variable, and was therefore discarded. A fast absorption profile has been documented for *S*-ketamine and the use of a first order process not only captured the quick absorption process but was also favorable for our model because it helped to avoid over-parametrization when the final DDI model was run with a complete dataset.

The use of semi-mechanistic pharmacokinetic modeling approach with hypothetical gut wall, portal vein and liver compartments allowed more physiological basis to evaluate the metabolism of *S*-ketamine to norketamine at the enzyme sites in the gut wall and liver. Our model resembled physiological biotransformation by taking into account individual variability in the blood flow, which was allometrically scaled using individual body weights. The metabolic process at the liver was coded in a way that it harnessed both first pass as well as circulatory extraction.

Plasma concentrations were converted to blood concentrations by multiplying plasma concentrations by the respective blood/plasma portioning ratio to allow physiological scaling using individual specific blood flow. We assumed these ratios to be constant across study participants. *S*-ketamine has a low plasma protein binding in humans (i.e. approximately 30%), and a recent

study has reported the blood: plasma partitioning ratio of 0.50 for *S*-ketamine in humans. Biological plausibility and previous evidence from the literature were the most important considerations, while making any changes in the model structure and only the changes that were relatable to human physiology, and were consistent with the literature were added to the models.

At first, a liver compartment was added into the *S*-ketamine model assuming no effusion delays and active transports, using a well stirred clearance model which was specified as,

$$F_{H,SK} = 1 - E_{H,SK} = 1 - \frac{f_{u,SK} \cdot CL_{INT,H,SK}}{Q_H + (f_{u,SK} \cdot CL_{INT,H,SK})} = \frac{Q_H}{Q_H + (f_{u,SK} \cdot CL_{INT,H,SK})}$$

where $F_{H,SK}$ is the hepatic availability of *S*-ketamine, $E_{H,SK}$ is portion of *S*-ketamine that is metabolized in the liver (i.e. extraction), $f_{u,SK}$ is the fraction of *S*-ketamine unbound in the liver, and $CL_{INT,H,SK}$ is the intrinsic hepatic clearance, Q_H is the blood flow parameter specifying the physiological blood flow of liver in the human body that was calculated specifically for each individual using allometric scaling of body weight (i.e. $Q_H = 3.75 \cdot WTKG^{0.75}$). An inter-individual variability parameter was included for intrinsic hepatic clearance in our model.

Metabolic enzymes are present at the villous tips in the intestine[1,2]. Therefore the gut wall extraction represents an example of true first pass metabolism in humans, by contributing to the overall drug elimination in the human body during the absorption phase only. In contrast, the portal vein compartment served essentially as a transit compartment for the *S*-ketamine model between gut wall and liver compartments, and was also connected to the central compartment in the mammillary three compartmental system to receive drug input via physiological portal blood flow.

It has been documented in the literature that CYP3A enzymes are also involved in the metabolism of *S*-ketamine *in vivo*[3]. Previous results show that the amount of CYP2B6 in the gut wall compartment is negligible as compared to liver[4], hence the intrinsic clearance at the gut wall is completely relatable to CYP3A4 contribution to *drug* metabolism. We implemented a well-stirred model also at the gut wall site to describe intestinal first pass metabolism to account for CYP3A dependent metabolism. The gut wall clearance was coded into the model as,

$$F_{GW,SK} = 1 - E_{GW,SK} = 1 - \frac{f_{u,GW,SK} \cdot CL_{INT,GW,SK}}{Q_{GUT} + (f_{u,GW,SK} \cdot CL_{INT,GW,SK})} = \frac{Q_{GUT}}{Q_{GUT} + (f_{u,GW,SK} \cdot CL_{INT,GW,SK})}$$

where $F_{GW,SK}$ is the availability of *S*-ketamine in the gut wall, $E_{GW,SK}$ is the portion of *S*-ketamine that is metabolized in the gut wall, $f_{u,GW,SK}$ is the fraction unbound in the gut wall (fixed to 1), and $CL_{INT,GW,SK}$ is the intrinsic gut wall clearance of *S*-ketamine, Q_{GUT} is the blood flow parameter specifying the physiological blood flow of gut wall in the human body.

In conjunction, the Q_{GUT}-model[5] was implemented into the gut wall well stirred clearance model. It follows the well-stirred clearance model and uses a hybrid parameter of the villous blood flow and permeability clearance of the drug to calculate a physiological blood flow towards gut wall in humans. The use of a Q_{GUT}-model for *S*-ketamine was necessitated by the fact that the permeability clearance of *S*-ketamine is low as compared to the value of villous blood flow ($Q_{VI} \gg CL_P$). Therefore the value of Q_{GUT} for *S*-ketamine approaches the value of permeability clearance.

The value for the permeability clearance of *S*-ketamine across human gut mucosa could not be found in previously published literature, a recent study has documented the value of apparent permeability (P_{app}) of *S*-ketamine using the Parallel artificial membrane permeability (PAMPA) assay[6]. A value of 1.49 ± 0.04 ($\times 10^{-6}\ cm/s$) at a pH of 6.5 has been reported and was used to calculate the value of permeability clearance (CL_p) of *S*-ketamine through the gut wall mucosa using the previously published equation for the effective intestinal permeability in man ($P_{eff,man}$)[5],

$$logP_{eff,man} = 0.45 \times logP_{PAMPA,pH\ 6.5} + 0.16$$

$$P_{eff,man} = 1.74 \times 10^{-4}\ cm/s$$

Then,

$$CL_p = P_{eff,man} \times A$$

where

CL_p is the permeability clearance across gut wall mucosa and A is the surface area of the small intestine in humans, numerically calculated in the literature[5] to be 0.66 m^2.

Hence,

$$CL_p = (1.74 \times 10^{-4}) * 6600 = 1.15\ cm^3/s = 4.1\ L/hr$$

A value of 4.1 L/hr was used for the permeability clearance of *S*-ketamine in humans, using the Q_{GUT} model as follows,

$$Q_{GUT} = Q_{VI} \times \frac{CL_P}{Q_{VI}} + CL_P$$

where Q_{VI} is the physiological villous blood flow was defined as:

$$Q_{VI} = Q_H + Q_{INT} + Q_{MU} \ = (3.75 \times\ 65.3^{0.75}) \times\ 0.4 \times 0.8 \times 0.6 = 16.5\ L/hr$$

$$Q_{GUT} = \mathbf{3.24} \cong\ CL_P$$

As it was implied via the calculations that the value of Q_{GUT} for *S*-ketamine approaches the value of CL_P in humans, therefore a Q_{GUT} model was implemented in the gut wall well stirred clearance model. In addition, an assumption was made in the modeling process that *S*-ketamine is metabolized in the human body via only one metabolic pathway, i.e. CYP2B6 mediated N-oxidation to norketamine. This assumption allowed us to use the eliminated amount of *S*-ketamine as input to the metabolite model without the need of assigning a fractional parameter, which also helped in developing DDI model later on.

The simplified *quasi steady state approximation*[7] approach introduced by Brill et al. 2016[8] was used in the specification of differential equations for model specifications. The derivation of these model equations can be obtained from the supplementary materials of the original article. The model equations for *S*-ketamine are as follows,

$$\frac{dA_{depot}}{dt} = -\frac{K_{a,SK} \cdot A_{depot}}{\frac{Q_{VI}}{V_{GW}}}$$

$$A_{GW,SK} = \frac{K_{a,SK} \cdot\ A_{depot}}{\frac{Q_{VI}}{V_{GW}}}$$

$$A_{PV,SK} = \frac{\frac{Q_{VI}}{V_{GW}} \cdot F_{GW,SK} \cdot A_{GW,SK} + \frac{Q_{PV}}{V_{C,SK}} \cdot A_{C,SK}}{Q_{PV}/V_{PV}}$$

$$A_{H,SK} = \frac{\frac{Q_{HA}}{V_{C,SK}} \cdot A_{C,SK} + \frac{Q_{PV}}{V_{PV}} \cdot A_{PV,SK}}{Q_H / V_H}$$

$$\frac{dA_{C,SK}}{dt} = \frac{F_{H,SK} \cdot Q_H \cdot A_{H,SK}}{V_H} - \frac{(Q_{HA} + Q_{PV} + Q_{1,SK} + Q_{2,SK}) \cdot A_{C,SK}}{V_{C,SK}} + \frac{Q_{1,SK} \cdot A_{P1,SK}}{V_{P1,SK}} + \frac{Q_{2,SK} \cdot A_{P2,SK}}{V_{P2,SK}}$$

$$\frac{dA_{P1,SK}}{dt} = \frac{Q_{1,SK} \cdot A_{C,SK}}{V_{C,SK}} - \frac{Q_{1,SK} \cdot A_{P1,SK}}{V_{P1,SK}}$$

$$\frac{dA_{P2,SK}}{dt} = \frac{Q_{2,SK} \cdot A_{C,SK}}{V_{C,SK}} - \frac{Q_{2,SK} \cdot A_{P2,SK}}{V_{P2,SK}}$$

where $K_{a,SK}$ is the first order absorption rate constant of *S*-ketamine, A_{depot}, $A_{GW,SK}$, $A_{PV,SK}$, $A_{H,SK}$, $A_{C,SK}$, $A_{P1,SK}$ and $A_{P2,SK}$ are the amounts of *S*-ketamine in depot, gut wall, portal vein, liver, central, 1st peripheral, and 2nd peripheral compartments respectively. V_{GW}, V_{PV}, V_H, $V_{C,SK}$, $V_{P1,SK}$, and $V_{P2,SK}$ are the volumes of gut wall, portal vein, liver, central, 1st peripheral, and 2nd peripheral compartments respectively. Q_{VI}, Q_{PV}, and Q_{HA}, and Q_H are the blood flows of gut wall, portal vein, hepatic artery and liver respectively. $F_{GW,SK}$ and $F_{H,SK}$ are the gutwall and hepatic availabilities of *S*-ketamine respectively. $Q_{1,SK}$ and $Q_{2,SK}$ are the distributional clearances to the 1st and 2nd peripheral compartments respectively.

Norketamine model

Similarly to *S*-ketamine, model building for norketamine was also done in a stepwise manner via which nested models were developed with the ultimate goal of creating a semi-PBPK model like the parent drug. A two compartment model was noticed to best describe the disposition kinetics of norketamine (ΔOFV = -734). A three compartmental mammillary model did not improve the model fit significantly (ΔOFV = -2) and the parameter estimates for the third peripheral volume and distributional clearance was observed to have a high uncertainty value (%RSE > 100%).

It was assumed that *S*-ketamine is only metabolized to norketamine *in vivo*. This assumption is biologically plausible since approximately 80% of *S*-ketamine is metabolized to norketamine[3,9] and therefore the extraction of the parent drug at the gut wall and liver metabolic sites were used as direct inputs into the metabolite model without any scaling. This simplified the model and assisted in model estimations. Norketamine is known to be metabolized rapidly in humans to 6-hydroxynorketamine[10], and a well stirred clearance model was implemented at the gut wall and hepatic sites for norketamine.

The hepatic well stirred clearance model for norketamine was specified as,

$$F_{H,NK} = 1 - E_{H,NK} = 1 - \frac{f_{u,NK} \cdot CL_{INT,H,NK}}{Q_H + (f_{u,NK} \cdot CL_{INT,H,NK})} = \frac{Q_H}{Q_H + (f_{u,NK} \cdot CL_{INT,H,NK})}$$

where $F_{H,NK}$ is the hepatic availability of norketamine, $E_{H,NK}$ is portion of norketamine that is metabolized in the liver (i.e. extraction), $f_{u,NK}$ is the fraction of norketamine unbound in the liver, and $CL_{INT,H,NK}$ is the intrinsic hepatic clearance, Q_H is the blood flow parameter specifying the physiological blood flow of liver in the human body.

In addition, the gut wall well stirred clearance model was coded into the model as follows,

$$F_{GW,NK} = 1 - E_{GW,NK} = 1 - \frac{f_{u,GW,NK} \cdot CL_{INT,GW,NK}}{Q_{VI} + (f_{u,GW,NK} \cdot CL_{INT,GW,SK})} = \frac{Q_{VI}}{Q_{VI} + (f_{u,GW,NK} \cdot CL_{INT,GW,NK})}$$

where $F_{G,NK}$ is the availability of norketamine in the gut wall, $E_{G,NK}$ is the portion of norketamine that is metabolized in the gut wall, $f_{u,G,NK}$ is the fraction unbound in the gut wall (fixed to 1), and $CL_{INT,G,NK}$ is the intrinsic gut wall clearance of norketamine, Q_{VI} is the blood flow parameter specifying the physiological blood flow of gut wall villi in the human body.

In comparison to *S*-ketamine, Q_{GUT} model was not implemented for the metabolite, and instead the villous blood flow was used in the gut wall clearance model. This was due to the fact that no value of permeability clearance or related parameters could be found in documented literature, and it was assumed that Q_{GUT} approached the physiological value of Q_{VI}[8].

The metabolite model was specified using the following equations,

$$A_{GW,NK} = (1 - F_{GW,SK}) \cdot A_{GW,SK}$$

$$A_{PV,NK} = \frac{\frac{Q_{VI}}{V_{GW}} \cdot F_{GW,NK} \cdot A_{GW,NK} + \frac{Q_{PV}}{V_{C,NK}} \cdot A_{C,NK}}{Q_{PV}/V_{PV}}$$

$$A_{H,NK} = \frac{\frac{Q_{HA}}{V_{C,NK}} \cdot A_{C,NK} + \frac{Q_{PV}}{V_{PV}} \cdot A_{PV,NK} + \frac{Q_H}{V_H} \cdot E_{H,SK} \cdot A_{H,SK}}{Q_H/V_H}$$

$$\frac{dA_{C,NK}}{dt} = \frac{F_{H,NK} \cdot Q_H \cdot A_{H,NK}}{V_H} - \frac{(Q_{HA} + Q_{PV} + Q_{1,NK}) \cdot A_{C,NK}}{V_{C,NK}} + \frac{Q_{1,NK} \cdot A_{P1,NK}}{V_{P1,NK}}$$

$$\frac{dA_{P1,NK}}{dt} = \frac{Q_{1,NK} \cdot A_{C,NK}}{V_{C,NK}} - \frac{Q_{1,NK} \cdot A_{P1,NK}}{V_{P1,NK}}$$

where $A_{GW,NK}$, $A_{PV,NK}$, $A_{H,NK}$, $A_{C,NK}$, and $A_{P1,NK}$ and are the amounts of norketamine in gut wall, portal vein, liver, central, and 1st peripheral respectively. V_{GW}, V_{PV}, V_H, $V_{C,NK}$, and $V_{P1,NK}$ are the volumes of gut wall, portal vein, liver, central, and 1st peripheral compartment respectively. Q_{VI}, Q_{PV}, and Q_{HA}, and Q_H are the blood flows of gut wall, portal vein, hepatic artery and liver respectively. $F_{GW,NK}$ and $F_{H,NK}$ are the gutwall and hepatic availabilities of norketamine respectively. $\cdot E_{H,SK}$ is the extraction of *S*-ketamine from the liver, $Q_{1,NK}$ is the distributional clearance of norketamine to the 1st peripheral compartment.

Ticlopidine model

For ticlopidine, model development started with an empirical one compartmental model. A two compartmental model was noticeably better than a one compartmental model (ΔOFV = -141), while a three compartmental model could not be fitted successfully to the data at hand, and thus was discarded. Due to sparsity in the early absorption phase of ticlopidine, the absorption rate constant had to be fixed to the literature value of 3.3/hr[11]. Likewise *S*-ketamine; gut wall, portal vein and liver compartments were added to the ticlopidine model in a sequential manner to replicate physiological metabolism at these sites.

The primary challenge in ticlopidine model development was to adequately fit the sparsely sampled absorption. Fixing the absorption rate constant to the previously published value stabilized the model but a high level of uncertainty across model parameters questioned the validity of the model. Therefore, different approaches to account for ticlopidine absorption were tried. A transit compartmental model was attempted via which transits were added ahead of the gut wall compartment in a sequential manner to optimize the number of transits needed. Interestingly, a four transit compartment model alongside gut wall, portal vein and liver compartments with a two compartmental distributional model resulted in a good model fit (ΔOFV = -36) and significantly reduced the uncertainty in model parameters.

Both the gut wall and hepatic clearances of ticlopidine were specified using a well stirred clearance model at these sites as follows,

$$F_{GW,TIC} = 1 - E_{GW,TIC} = 1 - \frac{f_{u,GW,TIC} \cdot CL_{INT,GW,TIC}}{Q_{VI} + (f_{u,GW,TIC} \cdot CL_{INT,GW,TIC})} = \frac{Q_{VI}}{Q_{VI} + (f_{u,GW,TIC} \cdot CL_{INT,GW,TIC})}$$

$$F_{H,TIC} = 1 - E_{H,TIC} = 1 - \frac{f_{u,TIC} \cdot CL_{INT,H,TIC}}{Q_H + (f_{u,TIC} \cdot CL_{INT,H,TIC})} = \frac{Q_H}{Q_H + (f_{u,TIC} \cdot CL_{INT,H,TIC})}$$

where $F_{GW,TIC}$ and $F_{H,TIC}$ are the hepatic and gut wall availability of ticlopidine respectively, $E_{GW,TIC}$ and $E_{H,TIC}$ are the portions of ticlopidine that are metabolized in the gut wall and liver respectively (i.e. extraction), $f_{u,GW,TIC}$ and $f_{u,TIC}$ are the fraction of ticlopidine unbound in the gut wall and liver respectively, Q_H and Q_{VI} are the blood flow parameters specifying the physiological blood flow of liver and gut wall villi in the human body, and $CL_{INT,H,TIC}$ is the intrinsic hepatic clearance of ticlopidine.

Initially, we tried to calculate the gut wall clearance of ticlopidine freely in the model estimations, however due to the sampling design of the original study, gut wall clearance could not be calculated as a model parameter and had to be fixed in the final model. Assuming the gut wall clearance of ticlopidine to be zero and liver as the only site of metabolism resulted in a good model fit and was therefore added to the final model as such.

It has been documented that repeated ticlopidine dosing can lead to a markedly elevate its half-life in healthy human volunteers, and a similar phenomenon has also been observed in elderly patients. This points to a possible auto-inhibition of ticlopidine metabolism. The hypothesis is biologically plausible since ticlopidine is a potent inhibitor of CYP2B6, the enzyme that contributes to ticlopidine metabolism in humans. All attempts to model an auto-inhibition of ticlopidine metabolic clearance in our model were unsuccessful, and thereafter ticlopidine metabolism was described with a first order elimination process.

The use of a simplified *quasi steady state approximation approach* could not be warranted for the ticlopidine model since the simplification results in coding the gut wall, portal vein and liver compartments into the model as hypothetical compartments in the $DES block of NONMEM code. Such a specification could not be implemented for ticlopidine because the varying amounts of ticlopidine (inhibitor) were to be used as inputs for the drug-drug interaction model (also specified in the $DES block). The inhibitor concentrations were used to calculate reversible and time dependent variables of the mechanistic static model (see below). Therefore, rather than using a simplified approach, the ticlopidine semi-mechanistic model was hard coded using the specification used by Frechen et al. 2013[12].

The model equations used for ticlopidine are as follows,

$$\frac{dA_{depot,TIC}}{dt} = -K_{a,TIC} \cdot A_{depot,TIC}$$

$$\frac{dA_{GW,TIC}}{dt} = K_{a,TIC} \cdot A_{T_n} - \frac{E_{GW,TIC} \cdot Q_{VI} \cdot A_{GW,TIC}}{V_{GW}} - \frac{F_{GW,TIC} \cdot Q_{VI} \cdot A_{GW,TIC}}{V_{GW}}$$

$$\frac{dA_{PV,TIC}}{dt} = \frac{F_{GW,TIC} \cdot Q_{VI} \cdot A_{GW,TIC}}{V_{GW}} + \frac{Q_{PV} \cdot A_{C,TIC}}{V_{PV}} - \frac{Q_{PV} \cdot A_{PV,TIC}}{V_{PV}}$$

$$\frac{dA_{H,TIC}}{dt} = \frac{Q_{PV} \cdot A_{PV,TIC}}{V_{PV}} + \frac{Q_{HA} \cdot A_{C,TIC}}{V_{C,TIC}} - \frac{E_{H,TIC} \cdot Q_{H} \cdot A_{H,TIC}}{V_{H}} - \frac{F_{H,TIC} \cdot Q_{H} \cdot A_{H,TIC}}{V_{H}}$$

$$\frac{dA_{C,TIC}}{dt} = \frac{F_{H,TIC} \cdot Q_{H} \cdot A_{H,TIC}}{V_{H}} - \frac{Q_{PV} \cdot A_{PV,TIC}}{V_{PV}} - \frac{Q_{HA} \cdot A_{C,TIC}}{V_{C,TIC}} - \frac{Q_{PER1,TIC} \cdot A_{C,TIC}}{V_{C,TIC}} + \frac{Q_{PER1,TIC} \cdot A_{PER1,TIC}}{V_{PER1,TIC}}$$

$$\frac{dA_{PER1,TIC}}{dt} = \frac{Q_{PER1,TIC} \cdot A_{C,TIC}}{V_{C,TIC}} - \frac{Q_{PER1,TIC} \cdot A_{PER1,TIC}}{V_{PER1,TIC}}$$

$$\frac{dA_{T_{n-1}}}{dt} = K_{a,TIC} \cdot A_{depot} - K_{a,TIC} \cdot A_{T_{n-1}}$$

$$\frac{dA_{T_n}}{dt} = K_{a,TIC} \cdot A_{T_{n-1}} - K_{a,TIC} \cdot A_{T_n}$$

where $K_{a,TIC}$ is the first order absorption rate constant of ticlopidine, $A_{depot,TIC}$, $A_{GW,TIC}$, $A_{PV,TIC}$, $A_{H,TIC}$, $A_{C,TIC}$, $A_{P1,TIC}$, $A_{T_{n-1}}$ and A_{T_n} are the amounts of ticlopidine in depot, gut wall, portal vein, liver, central, 1st peripheral, $n-1th$ and nth transit compartment respectively. V_{GW}, V_{PV}, V_H, $V_{C,SK}$, $V_{P1,SK}$, and $V_{P2,SK}$ are the volumes of gut wall, portal vein, liver, central, and 1st peripheral compartments respectively. Q_{VI}, Q_{PV}, and Q_{HA}, and Q_H are the blood flows of gut wall, portal vein, hepatic artery and liver respectively. $E_{GW,TIC}$ and $E_{H,TIC}$ are the gut wall and hepatic extractions of ticlopidine respectively. $F_{GW,TIC}$ and $F_{H,TIC}$ are the gutwall and hepatic availabilities of ticlopidine respectively. $Q_{1,SK}$ is the distributional clearance to the 1st peripheral compartment.

Drug-drug interaction model

The development of drug-drug interaction (DDI) model was challenging because ticlopidine is a known mechanism based inhibitor of CYP2B6 enzyme, and unlike competitive inhibitors, the inhibition process requires specification using inhibitor concentrations and a mechanistic basis of enzyme degradation *in vivo*. Initial attempts to model the amount of enzyme resulted in poor model

performance, elicited by a high uncertainty around DDI model parameters. In context, a pseudo first order kinetic degradation model was also tried in an attempt to specify inhibitor dependent enzymatic degradation, which translated into an inhibition parameter that would cause a reduction in intrinsic hepatic clearance of *S*-ketamine at inhibitor phase. However, all these attempts were unsuccessful, and it was concluded that the amounts of enzyme could not be calculated with the data at hand.

The DDI model was then specified with a 'mechanistic static model (MSM)'[13]. This model has been and has also previously used by in an *in vitro* study to model ketamine-ticlopidine interaction[11]. According to the MSM model, the inhibition of CYP2B6 by ticlopidine is postulated to have a reversible and a time-dependent mechanism based components. Both of these components utilize the inhibitor concentration in the portal vein (I_{PV}) and CYP2B6 inhibition constants specific for ticlopidine. The reversible (competitive) component (A_H) of inhibition was calculated as follows:

$$A_H = \frac{1}{1 + \frac{[I_{PV}]}{k_i}}$$

where $[I_{PV}]$ is the concentration of the inhibitor i.e. ticlopidine at the portal vein (as specified in the model) which would account for the concentration of the inhibitor at the enzyme site in the liver, and k_i is the equilibrium dissociation constant of ticlopidine for CYP2B6. Secondly, the time-dependent non-competitive component (B_H) was specified:

$$B_H = \frac{k_{deg,H}}{k_{deg,H} + \frac{k_{inact} \cdot [I_{PV}]}{K_I + [I_{PV}]}}$$

where $k_{deg,H}$ is the physiological degradation rate of hepatic CYP2B6 at $[I_{PV}]$ = 0, $[I_{PV}]$ is the inhibitor i.e. ticlopidine concentration at the portal vein, k_{inact} is the maximum inactivation rate constant of ticlopidine for CYP2B6 as inhibitor concentration approaches infinity (i.e. true first-order inactivation rate constant) and K_I is the inactivator concentration at half maximal inactivation rate. Finally, the inhibition parameter describing the expected net effect on intrinsic hepatic clearance was calculated using A_H and B_H components for the interaction model as follows,

$$f_{CL'_{INT,H}} = \left(A_H \cdot B_H \cdot f_{m,CYP2B6}\right) + \left(1 - f_{m,CYP2B6}\right)$$

where $f_{CL'_{int,H}}$ is the inhibition parameter describing the fractional change in the intrinsic hepatic clearance of *S*-ketamine during the ticlopidine phase, and $f_{m,CYP2B6}$ is the fraction of *S*-ketamine metabolized by CYP2B6 in humans. Results from a recent in vitro study indicate that ticlopidine causes a 60% inhibition of *S*-ketamine metabolism. We performed a log-likelihood profiling for $f_{m,CYP2B6}$, using the llp-package in PsN toolkit and our result suggests a similar level of inhibition (i.e. 63%):

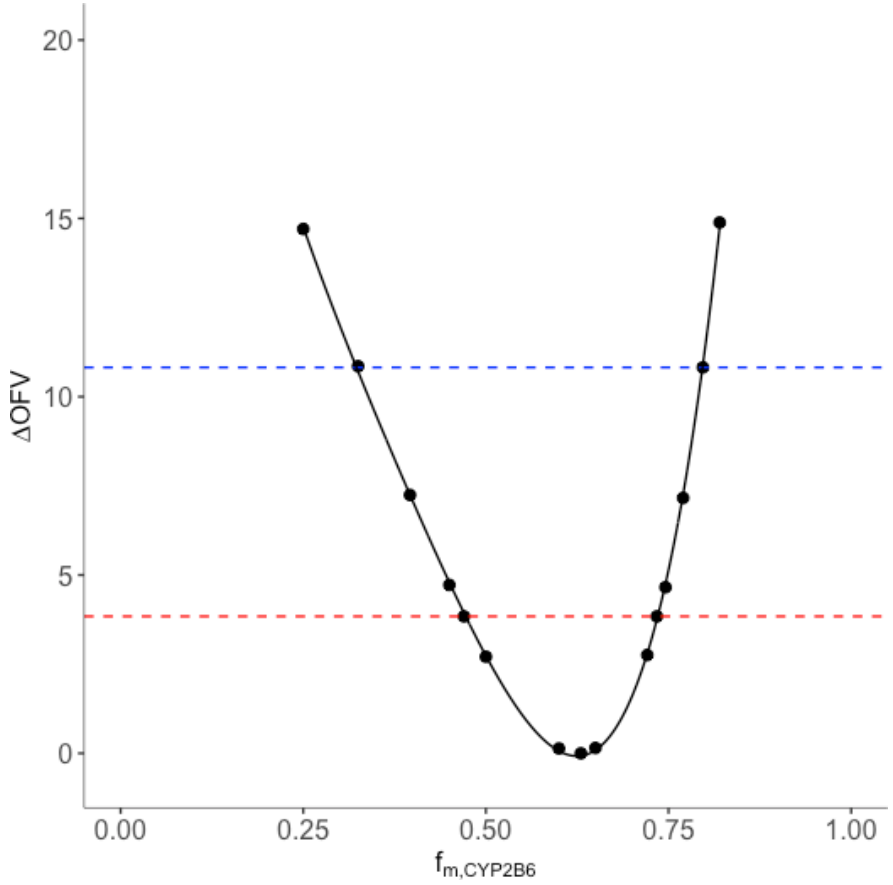

Figure S1**.** Log-likelihood profile of the fraction of *S*-ketamine metabolized by CYP2B6 ($f_{m,CYP2B6}$). Statistically significant values of the objective function value change are shown as red and blue dotted line for p<0.05 and p<0.01, respectively. ΔOFV, change in the objective function value.

A list of values for all parameters implemented in the inhibition model can be found in table 2. Lastly, the $f_{CL'_{int,H}}$ was used to calculate the effect of ticlopidine mediated CYP2B6 inhibition on the intrinsic hepatic clearance of *S*-ketamine:

$$CL_{INT,H,[I]} = CL_{INT,H,[I]=0} \cdot f_{CL'_{INT,H}}$$

$CL_{INT,H,[I]}$ and $CL_{INT,H,[I]=0}$ are the intrinsic hepatic clearance of *S*-ketamine during the ticlopidine and placebo phases, respectively. Gut wall clearances of *S*-ketamine and norketamine were calculated freely in the model parameter space.

The final DDI model specified using the MSM resulted in a good fit for *S*-ketamine pharmacokinetic profile at the ticlopidine phase. The model precisely predicted the fall in *S*-ketamine intrinsic hepatic clearance following ticlopidine pretreatment, which led to a rise in S-ketamine area under the curve (AUC) and maximum plasma concentration (Cmax). It was observed that the fall in intrinsic hepatic clearance represented an "on – off" phenomenon which seemed to be non-physiological and questioned model validity, but a simulation of model parameters showed that the concentration of ticlopidine required to cause a complete loss of enzyme activity is very low. Thereafter a fast buildup of ticlopidine concentration in the portal vein (i.e. *quasi steady state approximation approach*) led to a sharp fall in enzyme activity, which translated into a very steep decline in the intrinsic hepatic clearance.

In the original study[14], it was documented that ticlopidine does not cause any significant impact on norketamine profile and therefore no inhibition model was implemented for the metabolite. It was observed that the model could account for norketamine pharmacokinetic profile at the ticlopidine phase with a slight under-prediction. An inhibition model for norketamine metabolic clearance was not implemented because 1. The authors of the original article have not reported any change in metabolite profile upon inhibitor pre-treatment and, 2. The necessary information about the parameters of norketamine could not be found in documented literature.

The apparent under-prediction of norketamine AUC from the final model may be due to the reason that ticlopidine does affect the disposition profile of the metabolite in addition to the parent drug. Additionally, the large between-subject-variability in S-ketamine metabolism *in vivo*, the fast metabolism of norketamine to secondary metabolites, and the fact that there may be a very large variability in the enzyme levels (i.e. CYP2B6), which lie beyond the scope of the mechanistic static model, and may explain the apparent trends in norketamine model fit.

References

1. Murray GI, McFadyen MC, Mitchell RT, Cheung YL, Kerr a C, Melvin WT. Cytochrome P450 CYP3A in human renal cell cancer. *Br J Cancer*. 1999;79(11-12):1836-1842. doi:10.1038/sj.bjc.6690292.

2. Kolars JC, Lown KS, Schmiedlin-Ren P, et al. CYP3A gene expression in human gut epithelium. *Pharmacogenetics*. 1994;4(5):247-259.

3. Peltoniemi MA, Hagelberg NM, Olkkola KT, Saari TI. Ketamine: A Review of Clinical Pharmacokinetics and Pharmacodynamics in Anesthesia and Pain Therapy. *Clin Pharmacokinet*. 2016;55(9):1059-1077. doi:10.1007/s40262-016-0383-6.

4. Paine MF, Hart HL, Ludington SS, Haining RL, Rettie AE, Zeldin DC. the Human Intestinal Cytochrome P450 " Pie " Abstract : *Methods*. 2006;34(5):880-886. doi:10.1124/dmd.105.008672.was.

5. Yang J, Jamei M, Yeo KR, Tucker GT, Rostami-Hodjegan A. Prediction of intestinal first-pass drug metabolism. *Curr Drug Metab*. 2007;8(7):676-684. doi:10.2174/138920007782109733.

6. Keiser M, Hasan M, Oswald S. Affinity of Ketamine to Clinically Relevant Transporters. *Mol Pharm*. 2018;15(1):326-331. doi:10.1021/acs.molpharmaceut.7b00627.

7. Ingalls BP. *Mathematical Modeling in Systems Biology*. MIT Press; 2013.

8. Brill MJE, Valitalo PAJ, Darwich AS, et al. Semiphysiologically based pharmacokinetic model for midazolam and CYP3A mediated metabolite 1-OH-midazolam in morbidly obese and weight loss surgery patients. *CPT Pharmacometrics Syst Pharmacol*. 2016;5(1):20-30. doi:10.1002/psp4.12048.

9. Mion G, Villevieille T. Ketamine Pharmacology: An Update (Pharmacodynamics and Molecular Aspects, Recent Findings). *CNS Neurosci Ther*. 2013;19(6):370-380. doi:10.1111/cns.12099.

10. Hijazi Y, Boulieu R. Contribution of CYP3A4, CYP2B6, and CYP2C9 isoforms to N-demethylation of ketamine in human liver microsomes. *Drug Metab Dispos*. 2002;30(7):853-858. doi:10.1124/dmd.30.7.853.

11. Palacharla RC, Nirogi R, Uthukam V, Manoharan A, Ponnamaneni RK, Kalaikadhiban I. Quantitative in vitro phenotyping and prediction of drug interaction potential of CYP2B6 substrates as victims. *Xenobiotica*. 2017;0(0):1-13. doi:10.1080/00498254.2017.1354267.

12. Frechen S, Junge L, Saari TI, et al. A semiphysiological population pharmacokinetic model for dynamic inhibition of liver and gut wall cytochrome P450 3A by voriconazole. *Clin Pharmacokinet*. 2013;52(9):763-781. doi:10.1007/s40262-013-0070-9.

13. Fahmi OA, Maurer TS, Kish M, Cardenas E, Boldt S, Nettleton D. A combined model for predicting CYP3A4 clinical net drug-drug interaction based on CYP3a4 inhibition, inactivation, and induction determined in vitro. *Drug Metab Dispos*. 2008;36(8):1698-1708. doi:10.1124/dmd.107.018663.

14. Peltoniemi MA, Saari TI, Hagelberg NM, et al. Exposure to Oral *S*-ketamine is unaffected by itraconazole but greatly increased by ticlopidine. *Clin Pharmacol Ther*. 2011;90(2):296-302. doi:10.1038/clpt.2011.140.